

Laser interference as a lithographic nanopatterning tool

Cees J. M. van Rijn

Technical University of Delft
 Nano and Micro Engineered Structural
 Optimization
 SOCM Group
 Koiter Institute
 Mekelweg 2, 2628 CD Delft
 The Netherlands
 E-mail: c.j.m.vanrijn@wbmt.tudelft.nl

Abstract. Laser interference lithography is reviewed as an adequate nanopatterning tool for devices with periodic structures. The structure size may practically be chosen in the range between 100 nm and 10.0 μm by adjusting the angle of incidence θ of the incoming laser beam. The exposure method is fast, inexpensive, and applicable for large areas. The method may be used to fabricate microsieves, shadow masks, calibration grids, and photonic crystals. © 2006 Society of Photo-Optical Instrumentation Engineers. [DOI: 10.1117/1.2173269]

Subject terms: lithography; nanopatterning; laser interference; fabrication; lasers.
 Paper NP-12 received Mar. 1, 2005; revised manuscript received May 31, 2005; accepted for publication Jul. 1, 2005; published online Feb. 27, 2006.

1 Introduction

When two planar waves of coherent light interfere, a pattern of parallel fringes will appear. These fringes can be used for the exposure of a photosensitive layer.^{1,2} The depth of focus of this method is dependent on the coherence length of the light, and can be in the order of meters or more, compared to (sub)microns for conventional optical lithography systems.^{3,4} As a result, the demands on substrate flatness and wafer positioning are less critical.⁵

A double-exposure technique can be used to obtain a mesh-like pattern^{6–9} (see Fig. 1). After the first exposure, the substrate is rotated over 90 deg and exposed to laser interference lines again. Now the gratings cross each other, and after development, a square array of lacquer pores [Fig. 2(a)] remains. The exposure time of the photolacquer layer is a critical factor. In case a longer exposure time is chosen, a pattern as shown in Fig. 2(b) will be obtained. On further increase of the exposure time, isolated photolacquer dots [Fig. 2(c)] are formed.

2 Device Fabrication with Short Exposure Time

Part of an incoming plane wave is reflected by a mirror and interferes with the undisturbed part of the wave to form an interference pattern (grating) on the substrate surface. To produce the plane wave, TE polarized light of an argon laser with a wavelength λ_{uv} =351.1 nm is spatially filtered and expanded by focusing it on a pinhole (see Fig. 3).

If the light intensity of each beam is I_0 , the radiance on the surface is given by:

$$I = 4I_0 \sin^2\left(\frac{\pi x}{\Lambda_x}\right), \quad (1)$$

with Λ_x being the fringe period in the x direction planar to the photolacquer layer:

$$\Lambda_x = \frac{\lambda_{uv}}{2 \sin \theta}. \quad (2)$$

Here, λ_{uv} is the wavelength of the laser light in the medium that surrounds the substrate (usually air) and θ is the half-angle between the two beams. The smallest period that theoretically can be obtained is $\theta=90$ deg, which is equal to $\lambda_{uv}/2$, and for this configuration $\Lambda = \lambda_{uv}/2 = 175$ nm. The corresponding smallest pore size (with a porosity >30%) will be approximately $175/2 = 88$ nm. It is evident that at low porosity, smaller pore sizes can be made.

Since the beam is only split for a short path length near the substrate, this setup is very insensitive to mechanical instabilities, and no feedback loop¹² is required to stabilize the interference pattern. The thickness of the photosensitive layer needs to be chosen with care to avoid problems with the periodic pattern perpendicular to the substrate surface due to interference between the incoming beam and the one reflected on the substrate surface. Its period is given by $\Lambda_{\perp} = \lambda_{uv}/2n \cos \theta_n$, where n is the refractive index of the photoresist and $2\theta_n$ is the angle between the beams inside the resist. With $\theta=20$ deg and with $n=1.7$ at $\lambda_{uv} = 351.1$ nm, one finds $\Lambda = 510$ nm and $\Lambda_{\perp} = 105$ nm. Therefore, the thickness of the photoresist layer is chosen smaller than 105 nm. The area that can be patterned using a mirror of 2.5×2.5 cm² equals approximately 9×9 mm² for $\Lambda = 510$ nm.

The backside of a single crystalline 3-in. <100>-silicon wafer with a thickness of 380 μm is pre-etched to a thick-

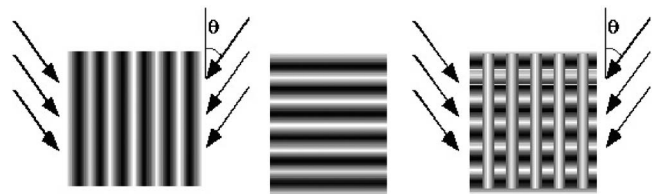
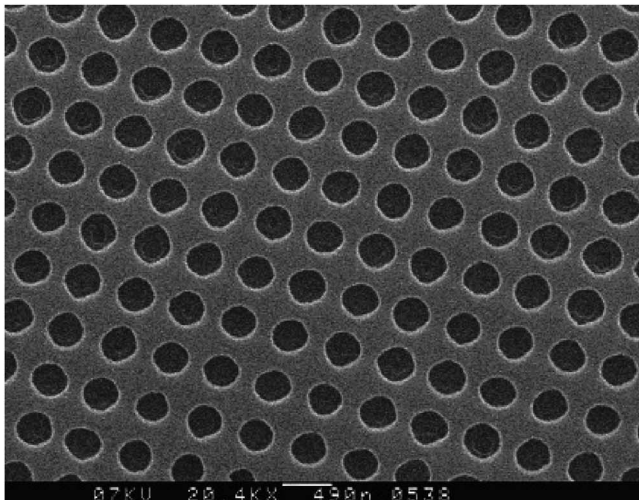
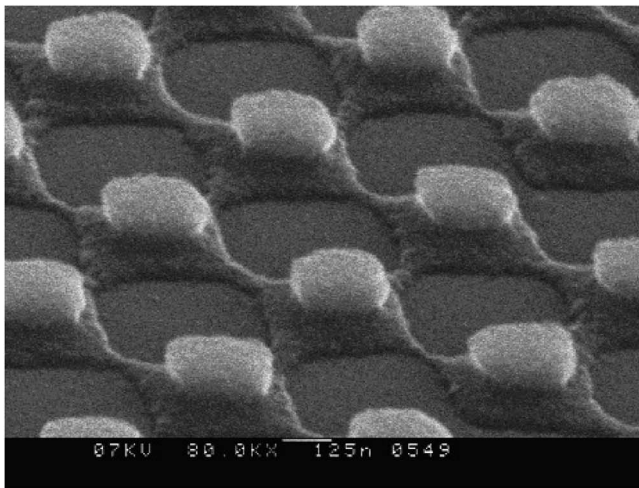


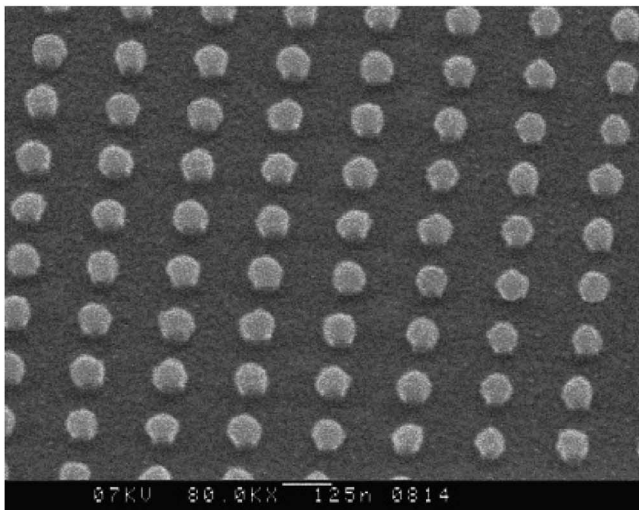
Fig. 1 (a) First exposure of the substrate with a photolacquer layer. (b) 90-deg rotation of the substrate. (c) Second exposure of the photolacquer layer.



(a)



(b)



(c)

Fig. 2 SEM micrograph of photolacquer layer that remains after a double exposure in the laser interference setup: (a) short exposure time, (b) intermediate exposure time [(a) and (b) reprinted with permission from the *Journal of Micromechanics and Microengineering*¹⁰] and (c) long exposure time (reprinted with permission from *Nanotechnology*¹¹).

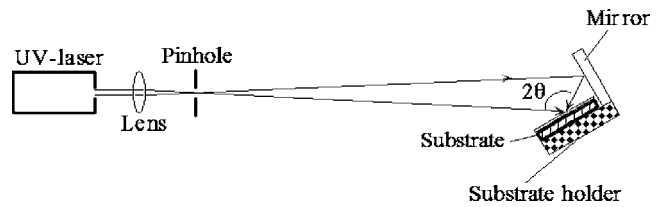


Fig. 3 Setup for laser interference lithography: Lloyd's mirror configuration.

ness of 15 μm using optical lithography and conventional KOH etching (25%, 70°C) (see Fig. 4). On the front side of the pre-etched support (1), a layer (2) of amorphous low stress¹³ silicon nitride with thickness 0.1 μm is deposited by means of low pressure chemical vapor deposition by reaction of dichlorosilane (SiH_2Cl_2) and ammonia (NH_3) at a temperature of 850°C. Except in the area where the microsieve pattern will be formed, an etch mask layer (3) of sputtered chromium with a thickness of 30 nm is deposited. On top of this chromium layer (3), a layer (4) of positive resist was spun and patterned using interference lithography. A 100-nm-thick layer (4) of positive photoresist (Shipley S1800-series) was spun, followed by a 5-min prebake at 90°C to evaporate the solvent. The resist was exposed to the interference line pattern for 45 s. The intensity of the incoming light in the exposed area was measured to be 2 mW/cm² for normal incidence ($\theta = 0$ deg). After rotating the substrate over 90 deg the exposure was repeated. The resist was developed for 15 s in a 1:7 mixture of Shipley-Microposit 351 developer and deionized water and dried by spinning.

The exposure time was chosen such that only at the crossings of the grid lines (after first and second exposure) does the resist receive enough energy to be removed completely after development. Therefore, a 2-D pattern of pores is created in the resist. A scanning electron micrograph (SEM) image of the exposed (2×45 s) and developed resist is given in Fig. 2(a). The diameter of the pores in the

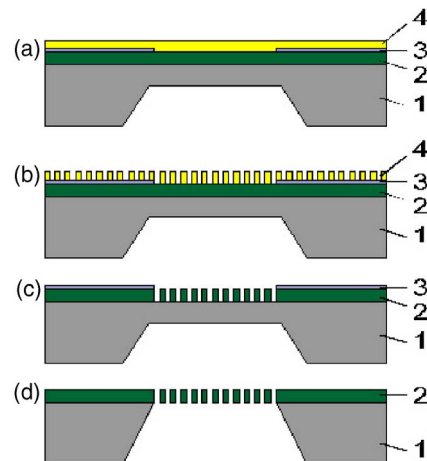


Fig. 4 Schematic representation of the fabrication process of a microsieve. The numbers indicate the silicon support (1), the silicon nitride membrane (2), the chromium etch mask (3), and the photoresist layer (4).

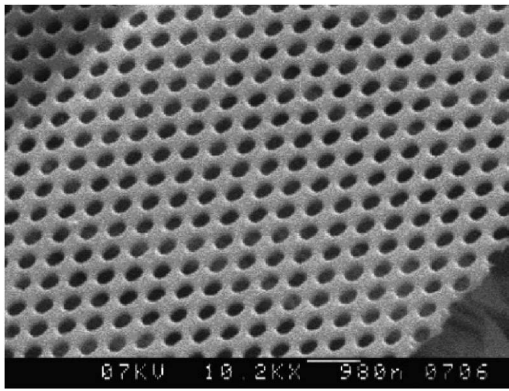


Fig. 5 SEM micrograph of the microsieve membrane showing pores with a diameter of 260 nm in a 100-nm-thick silicon nitride layer (reprinted with permission from *Nanotechnology*¹¹).

photoresist depends on the duration of exposure, giving a possible tool to vary the pore size at a constant pore-to-pore distance. However, when the exposure time chosen is too long (2×75 s), the pores in the resist pattern may become too large and will overlap [Fig. 2(b)].

Next, the interference pattern is transferred into the silicon nitride membrane layer (2) by means of CHF_3/O_2 reactive ion etching at 10 mTorr and 75 W for 2 min, forming the required perforations. Subsequently, the silicon underneath the membrane layer (2) is anisotropically etched^{14,15} with an SF_6/O_2 plasma at 100 mTorr and 100 W for 10 min with an etch rate of $2 \mu\text{m}/\text{min}$ to form the macroscopic openings in the support (1). Figure 5 shows a SEM photograph of the resulting perforated membrane layer (2) showing a very regular pore pattern, the pore size being 260 nm with a pore-to-pore spacing of 510 nm. The pore size was very uniform over the whole $9 \times 9\text{-mm}^2$ area.

3 Short Versus Long Laser Interference Exposure Times

For the fabrication of microsieves, an array of pores is needed. Such an array can be obtained by a double exposure with an intermediate rotation over an angle α . For $\alpha = 90$ deg the array is square, and for $\alpha = 60$ deg it is hexagonal.¹⁶ After the second exposure, the photolacquer layer is developed, where the sum of the two exposure doses determines whether it dissolves in the developer. For a positive resist, the areas that receive a dose above a certain threshold dose will completely dissolve. For a certain (short) exposure time, only the areas where two intensity maxima overlapped will have received a total dose that exceeds the threshold value. These areas will dissolve during development, and an array of pores will appear in the resist layer. An SEM micrograph of such an array of pores is shown in Fig. 6.

The picture shows that the resist between the pores exhibits “saddle points,” due to the overlap of a minimum and a maximum. For longer exposure times, these saddle points will also dissolve in the development process. The result is then an array of posts on the places where two minima overlap. The transition from pores to posts occurs quite rapidly, as the difference in received dose between the cen-

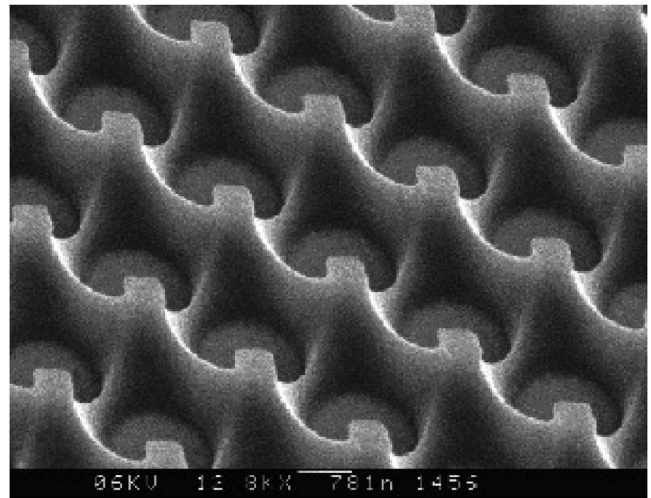


Fig. 6 Photolacquer layer after a double intermediate exposure time and subsequent development.

ter of a pore and a saddle point is only a factor of 2. The formation of posts is less critical. In theory, the posts will never disappear for increasing exposure times, as the received dose in the center of a post is always zero. The exposure process for a double-exposed resist layer for $\alpha = 90$ deg is explained next.

The contour lines in Fig. 7 are equidose lines and have been plotted on a logarithmic scale. This implies that, going from a bright region toward a dark region, the difference between two contour lines represents a decrease in received dose by a constant factor (in Fig. 7, this factor is $\sqrt{2}$). Suppose the first contour in a bright region (where a pore is formed) indicates the threshold dose. The photolacquer within this contour line will dissolve and an array of pores will appear. If the exposure time is increased by a factor of $\sqrt{2}$, the next (square-shaped) contour line will indicate the threshold dose. An array of large square pores will appear, which are almost interconnected. Another increase in exposure time leads to the next contour line, which represents

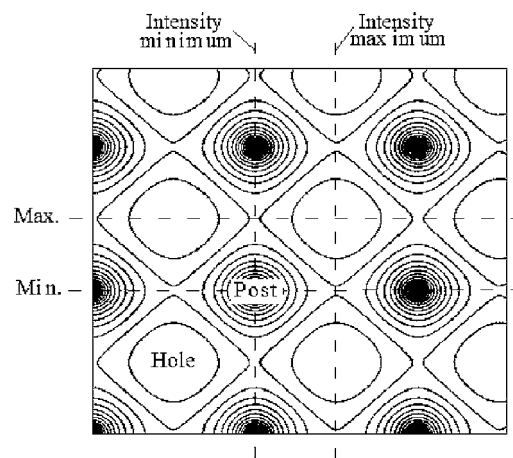


Fig. 7 Contour plot of the received dose of UV light in photolacquer layer exposed twice to a fringe pattern with an intermediate rotation over 90 deg (reprinted with permission from the *Journal of Micromechanics and Microengineering*¹⁷).

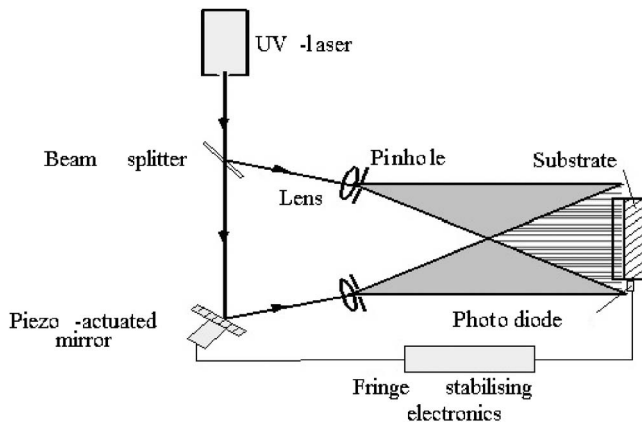


Fig. 8 Interference lithography setup for the exposure of large areas.

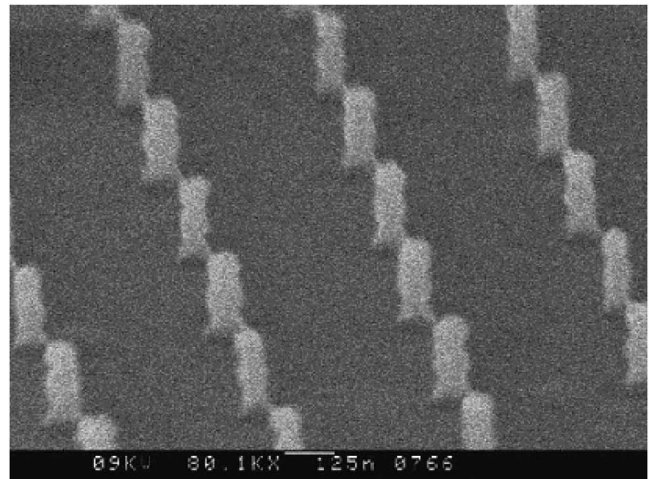
the contour of a post. A further increase in time leads to smaller posts, but the line density shows that the change in size of the posts is less dependent on a relative increase in dose than the change in size of the pores. In other words, the process latitude for the formation of posts is wider than for the formation of pores. This is important for the uniformity of the array, as in practice the laser light varies in intensity over the surface due to a Gauss distribution profile, the distance to the source, imperfect filtering, drift of the beam, and laser noise. To overcome the limitations of the pore-formation process, the postformation process can be used in combination with an image reversal method. Decker et al.¹⁸ used exposure doses for the creation of posts, but applied a base-catalyzed method before development to make the exposed areas insoluble. A subsequent flood exposure with a UV lamp made the previously unexposed parts soluble. The result was an array of pores in photolacquer produced with the wide process latitude of the postcreation method.

Pattern transfer from a photolacquer mask into a silicon nitride layer usually gives rise to tapered walls due to lateral etching of the mask. As tapered pores affect the filtration performance of membranes, an alternative process was developed. Posts were created and the pattern was inverted with a chromium lift-off process. 15 nm of chromium is evaporated onto the posts, which are then removed in an ultrasonic acetone bath. The remaining chromium forms a perforated layer. This layer serves as an etch mask for plasma etching. Pattern transfer into the silicon nitride using a chromium mask improves in comparison with a photolacquer mask, as the plasma hardly attacks the chromium.

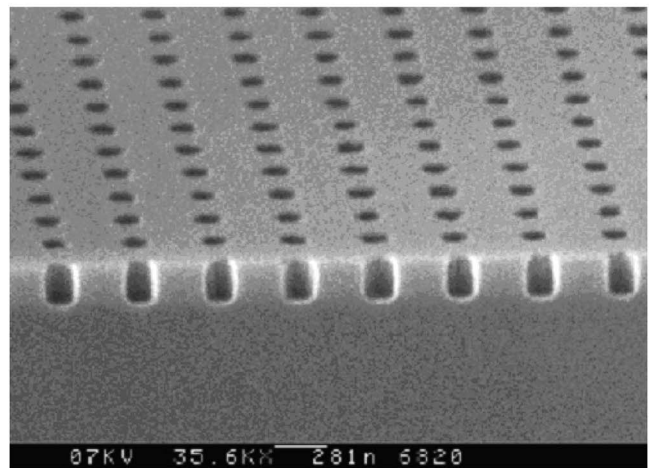
During exposure, the laser light partly reflects from the substrate and interferes with the incoming light. This causes the creation of an interference pattern in the vertical direction. The period Λ_z of this pattern is given by:

$$\Lambda_z = \frac{\lambda}{2n_{\text{res}} \cos \theta_{\text{res}}}, \quad (3)$$

where n_{res} is the refractive index of the photolacquer layer and θ_{res} is the angle of incidence in the resist.



(a)



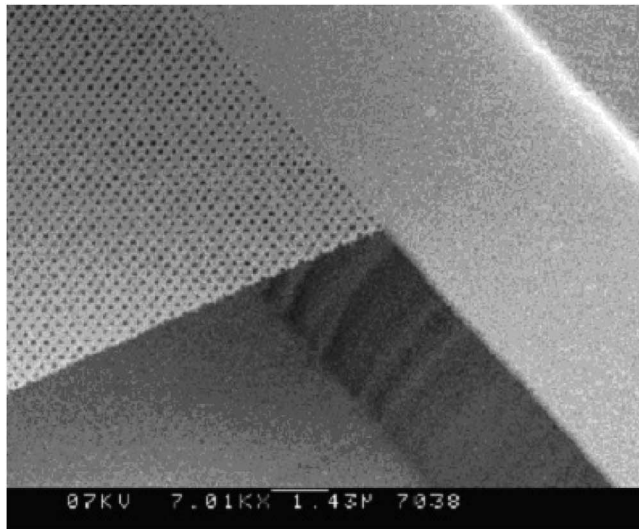
(b)

Fig. 9 (a) SEM micrograph of 80-nm-wide posts with rippled sidewalls caused by the vertical interference pattern. (b) SEM micrograph of a membrane after plasma etching through the pores in the chromium layer.

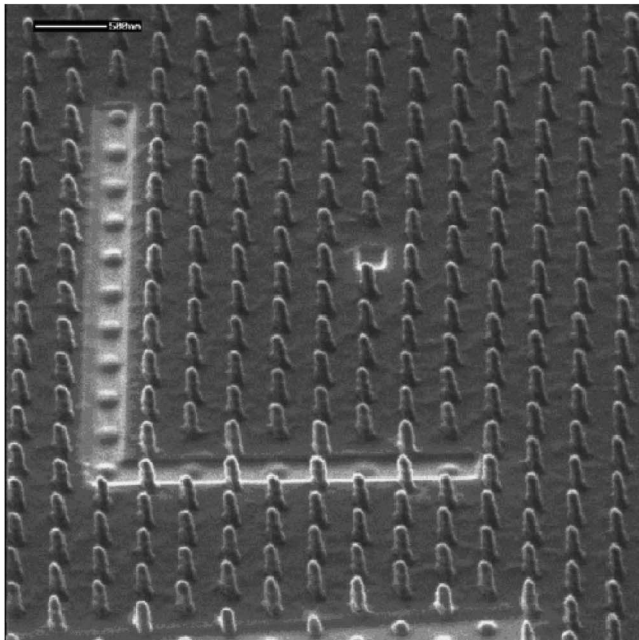
As a result of this vertical pattern, the posts will have a rippled sidewall, which makes the lift-off process more effective.

4 Experimental Setup

Part of an incoming plane wave reflects on the mirror and interferes with the undisturbed part of the wave to form an interference pattern (grating) on the substrate surface. To produce the plane wave, TE polarized light of an argon laser with wavelength $\lambda = 351.1$ nm is spatially filtered and expanded by focusing it on a pinhole. For large θ (small fringe periods), the system works satisfactorily, but for small θ , the image of the mirror on the substrate becomes so small that most of the substrate is not exposed to the interference pattern. An increase in mirror size is expensive, as the demands on smoothness and flatness are high. However, the setup is very useful for research purposes, as it is simple and θ can be changed easily by tilting the substrate holder. For the exposure of large surfaces, a second setup was built. In this setup the laser beam is split, after which both beams are expanded separately.



(a)



(b)

Fig. 10 SEM micrograph of a high-porosity microsieve made with the lift-off method for the production of photonic crystals (reprinted with permission from *Advanced Materials*²⁶), and SEM micrograph of a FIB-assisted removal of a number of pillar structures obtained with laser interference lithography (courtesy of Applied Optics Group, University of Twente).

As both beams travel long separate paths, the effects of vibration and air turbulence can easily disturb them. Therefore, a fringe-locking system is necessary. Fringes are detected by a photodiode, after which the signal is used by fringe stabilizing electronics to actuate a piezo element (see Fig. 8). Using a similar setup, Spallas et al.¹⁹ reported the fabrication of uniform photolacquer posts on a $50 \times 50\text{-cm}^2$ glass substrate. The setup is less sensitive to dust particles than Lloyd's mirror configuration, as there are no mirrors after filtering of the beams. However, it is

time consuming to change θ , because this requires movement of a spatial filter, after which the beam has to be aligned on the pinhole again.

5 Fabrication

A silicon wafer was coated with a $0.5\text{-}\mu\text{m}$ -thick silicon-rich nitride layer to obtain a low-stress membrane.¹³ On top of this, a 250-nm -thick positive photolacquer layer (one part Shipley 1805 diluted with one part Microposit thinner) was spun at 4000 rotations per minute. Using Lloyd's mirror configuration with $\theta=20.55$ deg, a postpattern with period $\Lambda_x=500$ nm was obtained.

Various exposure times led to posts of different diameters. The smallest posts obtained are shown in Fig. 9. A further increase in exposure time led to posts falling over. The rippled sidewalls show about two periods of the vertical interference pattern in the 250-nm -thick layer. Calculation with Eq. (3) and $n_{\text{resist}}=1.7$ gives a period of 106 nm. After chromium lift-off, i.e., the removal of the posts covered with chromium, the pattern was etched into the silicon nitride membrane using a CHF_3/O_2 plasma (Fig. 9).

With the double-beam setup, microsieves were fabricated successfully using 3-in. wafers (see Fig. 10). Microsieves with pore sizes down to 65 nm were fabricated using double-exposure laser interference lithography. The pores are obtained with an inverse process, as the direct process of pore formation in photolacquer has narrow process latitude. An array of posts is transferred into an array of pores by evaporating chromium onto the posts, followed by a lift-off in acetone. The resulting patterned chromium layer is used as an etch mask for plasma etching of the silicon nitride membrane. The method is fairly robust, as the lift-off process exploits the rippled sidewalls of the posts to allow the acetone to dissolve the photolacquer. The laser interference lithography method has been used for the production of filtration membranes,^{20,21} shadow masks,^{22,23} SEM calibration grids, and photonic crystals.^{24,25}

Calibration grids can be obtained with two separate laser interference exposures on two subsequently applied photolacquer layers.

6 Conclusions

Microsieves with submicron pore sizes can be made using multiple laser interference lithography. The pore size may practically be chosen in the range between 100 nm and $10.0\ \mu\text{m}$ by adjusting the angle of incidence θ of the incoming laser beams. The exposure method is fast, inexpensive, and applicable for large areas.

References

1. S. Austin and F. T. Stone, "Fabrication of thin periodic structures in photoresist," *Appl. Opt.* **15**, 1071–1074 (1976).
2. B. de A. Mello, I. F. da Costa, C. R. A. Lima, and L. Cescato, "Developed profile of holographically exposed photoresist gratings," *Appl. Opt.* **34**(4), 597–603 (1995).
3. E. H. Anderson, C. M. Horwitz, and H. I. Smith, "Holographic lithography with thick photoresist," *Appl. Phys. Lett.* **43**(9), 874–875 (1983).
4. L. Mashev and S. Tonchev, "Formation of holographic diffraction gratings in photoresist," *Appl. Phys. A* **26**, 143–149 (1981).
5. S. H. Zaidi and S. R. J. Brueck, "Multiple-exposure interferometric lithography," *J. Vac. Sci. Technol. B* **11**, 658–666 (1993).
6. C. J. M. van Rijn, "Membrane filter as well as a method of manufacturing the same," PCT Patent Application 95/1386026.
7. A. Fernandez, P. J. Bedrossian, S. L. Baker, S. P. Vernon, and D. R.

- Kania, "Magnetic force microscopy of single-domain cobalt dots patterned using interference lithography," *IEEE Trans. Magn.* **32**, 4472–4474 (1996).
8. X. Mai, R. Moshrefzadeh, U. J. Gibson, G. I. Stegeman, and C. T. Seaton, "Simple versatile method for fabricating guided-wave gratings," *Appl. Opt.* **24**, 3155–3161 (1985).
 9. J. P. Spallas, A. M. Hawryluk, and D. R. Kania, "Field emitter array mask patterning using laser interference lithography," *J. Vac. Sci. Technol. B* **13**, 1973–1978 (1995).
 10. C. J. M. van Rijn, W. Nijdam, S. Kuiper, G. J. Veldhuis, H. van Wolferen, and M. Elwenspoek, "Microsieves made with laser interference lithography for microfiltration applications," *J. Micromech. Microeng.* **9**, 170–172 (1999).
 11. C. J. M. van Rijn, G. J. Veldhuis, and S. Kuiper, "Nanosieves with microsystem technology for microfiltration applications," *Nanotechnology* **9**, 343–345 (1998).
 12. C. O. Bozler, C. T. Harris, S. Rabe, D. D. Rathman, M. A. Hollis, and H. I. Smith, "Arrays of gated field-emitter cones having 0.32 μm tip-to-tip spacing," *J. Vac. Sci. Technol. B* **12**, 629–632 (1994).
 13. J. G. E. Gardeniers, H. A. C. Tilmans, and C. G. C. Visser, "LPCVD silicon-rich silicon nitride films for applications in micro-mechanics studied with statistical experimental design," *J. Vac. Sci. Technol. A* **14**, 2879–2892 (1996).
 14. H. V. Jansen, M. J. de Boer, H. Wensink, B. Kloeck, and M. C. Elwenspoek, "The black silicon method VIII: A study of the performance of etching silicon using SF₆/O₂-based chemistry with cryogenical wafer cooling and a high density ICP source," *Microelectron. J.* **32**, 769–777 (2001).
 15. J. W. Bartha, J. Greschner, M. Puech, and P. Maquin, "Low temperature etching of Si in high density plasma using SF₆/O₂," *Microelectron. Eng.* **27**, 453–456 (1995).
 16. S. C. Kitson, W. L. Barnes, and J. R. Sambles, "The fabrication of submicron hexagonal arrays using multiple-exposure optical interferometry," *IEEE Photonics Technol. Lett.* **8**(12), 1662–1664 (1996).
 17. S. Kuiper, H. van Wolferen, C. J. M. van Rijn, W. Nijdam, and M. Elwenspoek, "Fabrication of microsieves with sub-micron pore size by laser interference lithography," *J. Micromech. Microeng.* **11**, 33–37 (2001).
 18. J. Y. Decker, A. Fernandez, and D. W. Sweeney, "Generation of subquarter-micron resist structures using optical interference lithography and image reversal," *J. Vac. Sci. Technol. B* **15**(6), 1949–1953 (1997).
 19. J. P. Spallas, R. D. Boyd, J. A. Britten, A. Fernandez, A. M. Hawryluk, M. D. Perry, and D. R. Kania, "Fabrication of sub-0.5 μm diameter cobalt dots on silicon substrates," *J. Vac. Sci. Technol. B* **14**, 2005–2007 (1996).
 20. M. Mulder, *Basic Principles of Membrane Technology*, Kluwer Academic, New York (1996).
 21. C. J. M. van Rijn, "Nano and Micro Engineered Membrane Technology," Elsevier, Amsterdam (2004).
 22. M. Kolbel, R. W. Tjerkstra, J. Brugger, C. J. M. van Rijn, W. Nijdam, J. Huskens, and D. N. Reinhoudt, "Shadow-mask evaporation through monolayer-modified nanostencils," *Nano Lett.* **2**(12), 1339–1343 (2002).
 23. J. W. Brugger, J. W. Berenschot, S. Kuiper, W. Nijdam, B. Otter, and M. Elwenspoek, "Resistless patterning of sub-micron structures by evaporation through nanostencils," *Microelectron. Eng.* **53**, 403–405 (2000).
 24. E. Yablonovitch and T. J. Gmitter, "Photonic band structure: the face-centered-cubic case," *Phys. Rev. Lett.* **63**, 1950 (1989).
 25. K. Inoue, M. Wada, K. Sakoda, A. Yamanaka, M. Hayashi, and J. W. Haus, "Fabrication of two-dimensional photonic band structure with near-infrared band gap," *Jpn. J. Appl. Phys., Part 2* **33**, L1463–L1465 (1994).
 26. L. Vogelaar, W. Nijdam, H. A. G. M. van Wolferen, R. M. de Ridder, F. B. Segerink, E. Flück, L. Kuipers, and N. F. van Hulst, "Large area photonic crystal clabs for visible light with waveguiding defect structures: Fabrication with FIB-assisted laser interference lithography," *Adv. Mater. (Weinheim, Ger.)* **13**, 1551–1554 (2001).



Cees J. M. van Rijn graduated from the Vrije Universiteit of Amsterdam in 1982 in solid state physics. He received his PhD degree on "Nuclear magnetic relaxation of polyelectrolyte solutions" from the University of Leiden. He has worked at Phillips Eindhoven and gained special expertise in semiconductor technology during the "Megachip" project (1986–1991). In the early 1992 he founded Aquamarijn Micro Filtration and initiated research on micro filtration membranes made with semiconductor technology at the MESA Research Institute. He is a founding father of Medspray (www.medspray.com) established in 2000 and Nanomi (www.nanomi.com) established in 2004. He is author and co-author of several publications in the *Journal of MEMS, Nanotechnology and Nanoletters*. Recently he published a book *Nano and Micro Engineered Membrane Technology* [Elsevier, Amsterdam (2004) ISBN 0.444–51489–9]. The book covers a broad spectrum of membrane science and technology, such as micro and nano filtration, biosensors, photonics, microbiology, controlled drug delivery, nanopatterning, micro contact printing, atomization, and emulsification. His current interest is in the field of nanowire biosensing (www.nanosens.nl). He is a senior researcher in the Structural Optimization and Computational Mechanics Group of Prof. Fred van Keulen at the Technical University of Delft.